SLAC-PUB-1246
(I)
May 1973

# A TIME OF FLIGHT TRIGGER SYSTEM FOR USE WITH THE SLAC 40 INCH HBC

W. M. Smart†, K. Moriyasu††, D. W. G. S. Leith,
W. B. Johnson, and R. G. Friday

Stanford Linear Accelerator Center
Stanford University, Stanford, California 94305

## ABSTRACT

A data acquisition system consisting of time of flight scintillation counters, associated electronics and a PDP-9 computer was developed and installed for use with the SLAC 40" hydrogen bubble chamber. The system was designed for optimum timing resolution subject to the limitations imposed by the HBC design and was used primarily to determine the momentum of a neutral beam of $K_L^o$ and neutrons, by measuring time of flight from a production target to the chamber. The system was also used to trigger the HBC camera only when a low momentum beam particle was recorded. This paper gives the details of the design and operation of the hardware and of the procedures necessary to incorporate the time of flight information into the more conventional bubble chamber picture analysis.

(Submitted to Rev. Sci. Instr.)

---

*Work supported in part by the U. S. Atomic Energy Commission.

†Now at the National Accelerator Laboratory, Batavia, Illinois.

††Now at the University of Washington, Seattle, Washington.

## I. Introduction

Traditionally most bubble chamber experiments in high energy physics have used beams of charged particles from magnetic transport systems which pass a very limited band of momenta and in most instances define the beam momentum more precisely than can be done with direct chamber measurements. Precise knowledge of the incident momentum allows the experimenter to study final states which contain one undetected neutral particle by using three of the energy-momentum conservation equations to find the momentum of the missing neutral system and the fourth equation as a constraint for testing kinematic consistency assuming a mass for the missing neutral.

By contrast, neutral beams have a well-known direction (defined by collimators) but generally populate a broad spectrum of momenta and possibly contain several different kinds of particle (eg., $K_L^o$, neutrons, and antineutrons). When incident upon a hydrogen bubble chamber, they offer a totally different set of final states than are available in charged beam hydrogen experiments; and when the momentum spectrum of one component can be well measured (as inferred from decays in the case of $K_L^o$), studies of various final states as a function of beam momentum can be carried out without the systematic uncertainties usually present in comparing a number of separate experiments. However, one kinematic constraint equation must be used to deduce the momentum of the beam, and thus final states with neutral particles cannot be kinematically constrained. This inevitable condition has impeded realization of the full potential of this class of experiments.

In the present paper we describe a technique used to measure the momentum of incident neutral particles by timing their flight from a production target to the interaction point in the chamber. Neutral particles were produced by impinging electrons from the SLAC linac accelerated in the "beam knockout" mode against

a beryllium target. In this mode of operation, only one rf bunch every 50 nsec is populated with electrons, and the charge contained is bunched in a pulse of duration $\sim 10$ picosecond. The arrival of these temporally sharp bunches at the production target was sensed by a "Beam Pick Off" detector. The SLAC 40-inch Hydrogen Bubble Chamber was used to detect tracks from the interactions, and a system of twelve scintillation counters which covered $\sim 12\%$ of the solid angle in the forward hemisphere was used to detect the arrival times of secondaries from interactions in the chamber. The nominal flight path from production target to chamber was 56.7 meters. The average resolution of the timing measurement, after applying various corrections, was $\sim \pm 0.5$ nsec; and the overlap of the counters provided two independent measurements for each particle over most of the acceptance of the system. Taken together, these two timing measurements translate into a resolution, $\Delta p/p$, of $\pm 3.1\%$ for $K_L^o$ of 2 GeV/c and $\pm 5.4\%$ for neutrons of 5 GeV/c, and varies as $(1 - \beta^2)^{-1}$ for lower momentum. In actual usage for neutron-induced interactions with a missing nucleon in the final state, the missing mass resolution was $\sim \pm 40$ MeV for incident momenta below 5 GeV/c.

In addition to direct determination of the incident beam momentum, the timing information can be used to trigger the flash selectively. The data in this system were collected using a PDP-9 computer and required about 1.6 msec of read-in time. The flash delay for the 40 inch HBC was 2.75 msec and thus allowed the PDP-9 about 1 msec of computing time to evaluate the timing data before deciding whether to flash the lights and accept the picture. By triggering the flash only when there was at least one beam particle more than 5 nsec slower than the prompt $\beta = 1$ time, the momentum spectrum for $K_L^o$ was enhanced by 40% for momenta below 2 GeV/c.

The paper divides into eleven sections. The apparatus is described in detail in Section II - V; the counter system (Section II); the beam and Pick Off system (Section III); the timing electronics (Section IV); and the PDP-9 system (Section V). The middle sections (IV through VIII) deal with the handling of the raw measurements: monitoring, calibration, and corrections; incorporation of the measurements into the picture analyzing system; logical selection and use of timing in kinematic fitting. Section IX details our testing of the measurements with events having three constraint fits and shows results for events with missing neutrals. Section X describes the use of the timing measurements to trigger the HBC flash.

## II. Counters

Twelve scintillators, 8-1/2" wide, 5" to 10" long and 1/2" thick were installed in the HBC vacuum tank just outside the hydrogen vessel as shown in Fig. 1. The scintillators overlap one another almost completely, so that a particle passing through the chamber wall will in general pass through two scintillators, yielding two independent signals. This feature has proved to be extremely valuable as explained later in this paper. A Ferranti Gallium Phosphide Diode type XP20 pulsed light source (for system checkout purposes) was installed on one 8-1/2" x 1/2" surface of each scintillator and the remainder of this surface was made light absorbing by covering it with a mixture of fine graphite powder in vacuum grease, backed by black paper. If light had been allowed to reflect off this back surface, the scintillation pulse would have been longer and the timing correspondingly less certain. The scintillation light was collected from the other 8-1/2" x 1/2" surface by a bundle of 10 mil coated plastic fiber optics (about 12 miles of fiber per counter) to a 2-1/4" diameter lucite rod. Using fiber optics has several advantages over more conventional materials. The counter assembly was manufactured (up to the dotted line in Fig. 1) before installation in the cluttered vacuum tank, instead of gluing plastic together in the restricted space available. Since light loss increases as a function of light pipe radius divided by bend radius, the fibers can be bent to a much smaller radius than a large plastic light pipe before light loss becomes serious. Finally, the flexible fibers allowed some motion between the lucite rod light pipe and the scintillator during chamber expansion, even though both were mounted on the relatively fixed vacuum tank. The Pilot M Scintillators with the fiber optics and a one foot length of lucite rod attached were supplied by New England Nuclear Corporation. Aluminum foil and tape wrapping was used for the scintillator and rod, while flexible lighttight bags made from 10 mil black polyethylene (or two 5 mil layers where

more flexibility was needed) were used to cover the fiber bundles.

The lucite rod went out the vacuum tank wall through a double-o-ring seal and then through a hole in the magnet yoke to an Amperex XP-1021 photomultiplier tube. The long rod (about 53") is required to get the PMT outside the 26 kG magnetic field of the HBC. Unfortunately this long light pipe both attenuated the scintillation light and provided flight paths of varying length (and hence time) for the remaining photons. Both these effects tend to degrade timing resolution. Even at this distance each PMT was shielded by four layers of magnetic shielding to keep the fringe field from affecting the timing and pulse charge from the PMT. The inner two shields were concentric $\mu$-metal cylinders 1/32" thick. The inner one was 9-3/4" long and 2-1/4" inside diameter and the outer one 12" long and 3" inside diameter. These were surrounded by 8 turns of 20 mil thick M-15 transformer iron, with masking tape separating the layers and finally by a 4" outside diameter steel cylinder 1/8" thick which also served as the support for the PMT base. A 10,000 amp magnet lead was located a few inches from one of the PMT's and it was shielded by wrapping it with 10 turns of 20 mil transformer iron, eliminating any effect of the magnetic field from this high current on the adjacent PMT.

The standard PA1021 tube bases, supplied by Amperex Electronic Corporation were used. These tube bases operated satisfactorily for the experiment described here, which accumulated over 700,000 bubble chamber expansions. However, they were left in place on the bubble chamber for more than 10 million additional expansions. This additional vibration broke many of the connections in the tube bases, so one should pot the bases in epoxy to prevent this problem in any similar long term future application. Prodeline 50 ohm 1/2" spir-o-line signal cable was used for the 142 foot run to the electronics, mainly because of its extremely low variation of signal propagation time with temperature, but also because of its low attenuation

of the high frequency PMT pulse. The median charge per PMT pulse available to the electronics was typically 200 picocoulomb, although this varied between 120 and 330 picocoulomb for the different PMT's. For hydrogen safety reasons the tube bases were enclosed in nitrogen purged plastic bags and the high voltage supply was interlocked with the bubble chamber hydrogen alarm circuits.

## III. Timing

This system was intended to be used primarily to measure momentum for a beam of neutral $K_L^o$ mesons and neutrons. This beam produced $K_L^o$ with a momentum spectrum that extended from 1 to 10 GeV/c though the majority of the flux was between 2 and 6 GeV/c [1] and is shown schematically at the top of Fig. 2. Sweeping magnets, $\gamma$ ray absorbers and collimators have been omitted from this schematic. The beam height was collimated to the height of the gap between the upper and lower sets of scintillators. The primary electron beam from the Stanford Linear Accelerator hit a beryllium target 56 meters upstream from the 40" HBC. Normally the accelerator produces a pulse of electrons 1.6 microseconds long consisting of very sharp 10 picosecond long bunches every 1/3 nanosecond. For this experiment, however, a beam knock out system was used just after the accelerator injector to remove almost all of these sharp bunches, leaving only one every 50 nanoseconds.

The arrival time of each of the approximately 32 bunches of electrons at the target was sensed by a Beam Pick Off mounted just after the beryllium target. This Pick Off was basically a high quality signal cable (7/8", foam insulated) with a matched and terminated 50 ohm extension. When the electron beam passed through the center conductor of the extension, electrons were knocked out of the conductor and a sharp positive pulse sent down the 367 foot cable to the electronics.

At the electronics this pulse was + 4 volt (for $0.6 \times 10^9$ electrons per bunch into the BPO) with a rise time of less than 0.2 nanoseconds.

The arrival time of those neutral beam particles which send charged interaction products out through the HBC walls is sensed by the scintillation counters. Since the scintillation counters generally overlap one another, each charged interaction product that goes through the counters causes two independent pulses to be sent to the electronics. The time difference between the beam pick off signal from the target and these signals from the PMT's is then directly related to the time of flight of the neutral beam particles for the 56 meter distance from target to interaction point.

## IV. Electronics

The primary function of the electronics was to measure the time difference between the beam pick off signal and PMT's and to store this information until it could be converted to digital form and read into the PDP-9 computer. However, the physical realities of the experiment and the timing circuits themselves required far more complexity in the electronics than this simple function implies.

It is not possible to measure time to a fraction of a nanosecond using digital electronics, but it can be done successfully using analog methods. A commercially available time to amplitude converter (TAC), the EG&G TH200A, was chosen for this experiment. In this device the time difference is measured by starting and stopping the charging of a capacitor from a constant current source. The voltage on the capacitor was then stored in a SLAC-built peak hold circuit until it could be multiplexed into an analog to digital converter and read into the computer. Besides providing the required accuracy the TH200A has versatile, built-in gating circuits which proved extremely valuable in setting up the electronics to meet the

requirements of the experiment. This method of time measurement has several restrictions which must be considered. First and most important is that the process of reading out the TAC capacitor voltage and then resetting the TAC circuits takes considerabley longer than the SLAC 1.6 microsecond beam pulse, so that only one time measurement could be made per beam pulse with each TAC. Second, because the method of measurement is analog, all power supply voltages to the TAC are critical. To maintain the desired timing accuracy we found it necessary to select and adjust the power supplies carefully to remove any short-term noise or oscillation or long term drift. After data taking had been completed it was discovered that simultaneous firing of two or more TAC's fed from the same power supply made a change in their outputs, equivalent to as much as 0.4 nanoseconds, relative to the output for operation of a single TAC. This effect was measured and then a correction was applied in the off-line analysis. A third problem was that pulse shapes in the high speed electronics in front of the TAC, particularly in coincidence circuits, can affect the time measurement. While such circuits were held to a minimum, some were required to meet the other requirements of the experiment. To account for any such effects as well as the actual responses of the various components used for each of the twelve timing circuits, it was considered vital to measure the response of each timing circuit for a known input.

To calibrate each timing circuit a fast rise time pulse was generated and then split with a passive voltage divider. One of these signals replaced the PMT signal, and the other was fed through a CAD037 (Science Accessory Corp) continuously adjustable delay (0 to 50 nsec) and then replaced the Beam Pick Off signal. The responses into the computer for delay settings from 0 to 45 nanoseconds (the usable range of the timing circuits) was measured at 0.5 nanosecond intervals and this calibration

data was used in off-line analysis.

Figure 3 shows the fast logic for a single counter. The PMT signal from each counter first goes into a fast discriminator, which is only gated open during the beam pulse, and then is used to start the TAC. The compicated handling of the Beam Pick Off signal from the target, shown in the figure, served to select the appropriate bunch for the stop signal and to extend the useful timing range of the TAC from 38 nsec to about 45 nsec. For those scintillators which overlapped, a ± 6.5 nsec coincidence was required before the inhibit signal to the TAC was removed, thus permitting the TAC to record the timing data. The physical construction of the 40 inch HBC virtually required that the lucite light pipes be installed as shown in Figure 1, parallel to the beam. Any charged particle travelling a significant length along the lucite light pipe generated sufficient Cerenkov light to use up that TAC with useless and confusing timing data. The coincidence requirement helped reduce this effect.

Previous timing tests at SLAC[2] have shown that if the total charge in the signal was recorded as well as the timing information, it could be used later in the off-line analysis to reduce the timing error significantly as well as to obtain a reasonably accurate estimate of the timing accuracy for each individual signal. To measure charge 10% of the PMT signal was split off by a voltage divider and sent to a linear gate. The 10 nsec gate signal was derived from the TAC Valid Start signal, insuring that only a pulse which acutally started the TAC was measured by the linear gate. The output was stored in a peak hold circuit (similar to the one used for the timing output) until it could be multiplexed into the analog to digital converter and read into the computer. These charge measuring circuits were calibrated by replacing the PMT signal input with several different-sized known signals from a pulser and measuring the response into the computer.

Considerable care had to be taken in setting up the fast electronics, particularly as to cable length and output pulse widths to insure proper operation. The signal cable lengths from the PMT to voltage divider were adjusted so that the time between a high energy particle through the center of the scintillator and the arrival of the signal at the voltage divider was equal for all twelve counters. Because the scintillators overlapped this could be done using cosmic ray coincidences. To verify that the correct Beam Pick Off signal was being used to stop the TAC's (i.e., not one from an earlier or later bunch) the accelerator was operated so that only one of the 32 bunches was accelerated and the expected relationship of the Beam Pick Off and PMT signals was observed.

Since several events could occur in one beam pulse (including two or more which sent charged secondaries into the same counter), it was desirable to record some additional information to aid in matching a particular event in the bubble chamber picture with the correct timing data. For each beam pulse a firing pattern (FPTN) consisting of a coincidence matrix of flip-flops was recorded. The beam pulse was divided into eight time periods of four bunches each. The columns of the matrix represented these time periods and the rows represented the coincidences between overlapping counters. (Since the two counters at the extreme ends of the array do not overlap another counter completely, the singles in these two were also recorded into the FPTN).

After 1/3 of the bubble chamber pictures were taken, a bunch scaler system was added which recorded precisely the bunch in which each TAC fired. The TAC Valid Stop output goes to logical 1 after an acceptable stop signal is received and remains there for several microseconds. This signal was used as an input to an EG&G C126 strobed coincidence unit which gated the Beam Pick Off signal into the appropriate Bunch Scaler, thus recording the remaining beam bunches

on the target. These data were used later in the off-line analysis to insure that all counters which were associated with a particular interaction, had in fact recorded their data in the same bunch. After the bunch scalers had been added, the FPTN was changed to record singles in each of the twelve counters during each of the eight beam time periods described above.

The analog data from the twelve TAC's and twelve linear gates was stored temporarily in SLAC-built peak hold circuits and then serially multiplexed into a Hewlett-Packard 6416A 12 bit (4096 channel) 200 MHz linear ramp analog digital converter.[3] This system gave approximately 40 channels per nanosecond in the timing cirucits with a measured timing resolution of the electronics into the computer of better than 70 picoseconds full width at one tenth maximum.

## V. Computer

A Digital Equipment Corporation PDP-9 computer was selected for the data logging, monitoring, and control tasks of this experiment. The on-line program from a similar experiment at SLAC, which also used a PDP-9, was borrowed for this experiment; however, this program required considerable modification to meet our needs. The on-line program was written in assembly language in order to fit into the 8192 word memory, but the smaller off-line calibration and equipment check-out programs were written mostly in Fortran to save programming time.

After each beam pulse the data collected by the electronics were read into the PDP-9 via two data channels. The output of the analog to digital converter was connected to the higher priority data channel, insuring that each analog voltage was converted at a fixed time after it was stored, thus eliminating the effect of any drift in the peak hold circuits. The digital data from the FPTN, bunch scalers, beam pulse intensity monitor, and HBC camera roll/frame

counter were serially read into the second data channel while the analog to digital converter was busy converting the next analog point. The data read-in time was 1.6 milliseconds, while the normal flash delay for the 40" HBC is 2.75 msec; this left sufficient time to execute several hundred PDP-9 instructions before making the decision to flash the lights and advance the film. About 30% of the HBC pictures in the run were taken in the triggered mode. For these triggered pictures a signal was sent from the computer to the HBC camera to flash the lights if one or more of the counters had times within prespecified limits as will be described later. After a few milliseconds delay, a digital word was read which showed whether or not the HBC camera had actually taken a picture. The data were then rearranged to the desired output format and transferred to the output buffer. When the output buffer was full a record was written on the output magnetic tape. This tape could be taken directly to the SLAC IBM 360/91 computer for further analysis and correlation with the data from the HBC pictures.

In addition to the above data for each beam pulse, periodically the PMT high voltage supply values and the currents in the beam sweeping and bubble chamber magnets were read into the computer and logged on the output tape. If the computer was busy processing the previous event or writing a record on the output tape, it gated off the electronics to prevent another data read-in until it was ready for it. A run control panel was interfaced into the PDP-9 to display the operating state of the computer and to permit the experimenter to start and stop data taking, end files and start new ones on the output tape, and so forth.

For monitoring the experiment on line the computer accumulated histograms of each analog quantity as well as a few histograms showing the operation of the firing pattern. Any of these histograms could be displayed on an oscilloscope (where they would be updated as the data came in) or printed out on the teletype.

Histograms could be cleared and histogram and triggering parameters changed via the teletype during the course of the experiment. Input and output buffers could also be printed out on the teletype to aid in checking out and debugging both the electronics and the computer. More details on the computer system and hardware are contained in Reference 3.

## VI. Corrections, Calibration and System Monitoring

The Gallium Phosphide Diode pulse light source installed on each scintillator proved to be extremely useful in checking for proper operation of virtually the entire time and pulse charge measuring system (only the Beam Pick Off target signal operation was not checked). A sharp high voltage pulse was generated in the experiment control room. Ten percent of this signal was taken off by a passive voltage divider and the remainder was sent to the HBC on a 1/2" spir-o-line cable. A voltage divider inside the HBC vacuum tank provided twelve outputs, one for each diode. Part of the signal retained in the control room generated a gate for the discriminators and the remainder after suitable delay and attenuation replaced the Beam Pick Off cable to provide a stop pulse for the timing circuits. The pulser data were read into the computer in the usual way and entered into the histograms, but the output to magnetic tape was inhibited. The data rate was limited by the computer analysis time to 17 pulses per second. About 10,000 events were collected in ten minutes of pulser operation, but 20 minutes were then required to print out the 24 histograms on the teletype. Typical timing distributions were about 1 nsec full width at half maximum. The positions of the timing and pulse charge peaks and the width of the timing peak were then compared with previous pulser runs. Since at least 1/2 hour was required, pulser runs were taken only when the accelerator beam or bubble chamber was off for some other reason, usually at about one day intervals.

The calibration of the timing circuits into the computer has been described above in the section on electronics. To measure time of flight for the neutral beam particles it is necessary to relate accurately at least one point of this time scale to a known time of flight in the beam. In theory this could have been done by measuring the appropriate cable lengths and propagation speeds and electronic circuit delays, but this is impractical to accomplish with the required accuracy of a fraction of a nonosecond. PMT transit time in particular would be extremely difficult to measure well. Instead we chose to measure the system response to beam particles known to have essentially $\beta = 1$. It was impractical to run electrons or photons in the beam, but high energy muons could be easily obtained by turning off the first two sweeping magnets. The third sweeping magnet, located just before the HBC, and the HBC magnet were left on to sweep out low energy muons and to spread out the beam to intercept all the scintillators. Two feet of additional lead were put in the beam to absorb the $K_L^o$'s and neutrons. About 25,000 events were then run into the system and recorded in both the on-line histograms and on the output magnetic tape. The on-line histograms gave an immediate rough measurement of $T_\mu$ to use in defining the timing limits for triggered running. The data on tape were used later in the off-line analysis, after correction for individual pulse charge, to establish a more accurate value for $T_\mu$.

In the off-line analysis a time correction and estimated resolution were obtained from the measured pulse charge for each recorded time by the following empirical formulas:

$$\text{Time Corrections} = \mu_1\rho + \mu_2\rho^2$$

$$\text{Resolution} = \nu_1 + \nu_2\rho$$

$$\text{where } \rho \sim \frac{1}{Q' + C}$$

Q' is proportional to the measured pulse charge, with the constant of proportionality chosen to make the Q' distribution for each counter peak at the same value. C is a common constant added to Q' to limit the size of $\rho$ if the measured pulse charge is small.

The $\mu$ and $\nu$ coefficients were determined empirically by fitting the time difference recorded in overlapping counters when a single high energy particle went through both scintillators. The problem of Cerenkov light pulses in the light pipes complicated this fitting procedure for data obtained with the $K_L^o$ beam, so we chose to use data from cosmic rays. About 120,000 cosmic ray timing events were recorded on magnetic tape at a rate of 20,000 events per hour with the beam cut off. The bubble chamber magnet remained on to duplicate the actual running conditions at the PMT's. The timing electronics were set up as described previously with the exception of the stop signal. Since only timing differences between overlapping counters were of interest in this data, all that was required of the stop signal was that it occur at approximately the right delay after the counter signals and that it be common to all the TAC's. The OR of the discriminator outputs of the 11 overlapping counters was used to replace the Beam Pick Off stop signal.

As can be seen from Figure 1, the six counters at the top of the chamber are arranged to give five overlapping pairs. For each pair, 3000 events (each consisting of the measured time difference for each counter) were selected. The $\mu$ and $\nu$ coefficients for each of the six counters were then fit simultaneously to maximize the likelihood function. A similar procedure was then used on the bottom set of counters.

The time correction thus determined for each counter was applied to the muon events, and these corrected data were histogrammed to determine the proper $T_\mu$ for each counter to be used with the corrected production timing data.

## VII. Handling and Analysis of the Events

In order to incorporate these timing measurements into the analysis cycle of the bubble chamber portion of the experiment, a number of changes had to be made in both the handling of the data and in the analyzing codes. The events were scanned and measured as in most bubble chamber experiments, and then the timing information appropriate to the entire picture was addended to the back of the measurement records on magnetic tape. Thus each event carried from the start the full information (timing, pulse charge, and firing pattern) collected by the PDP-9 during that beam burst.

Reconstruction and fitting of the events were accomplished using TVGP and SQUAW [4], with suitable modifications to handle the timing measurements. This choice was motivated largely by our familiarity with these codes; however, the generality of SQUAW in its treatment of kinematical fitting was extremely well-suited to accomodate this new data.

The first rather obvious change was to store the timing information in some convenient place in the reconstruction output record format. The Identification Information Block (Block 2, as it is called in TVGP) was enlarged by 120 bytes to accomodate the new information.

The next task was to extend the orbit of each measured track to discover those which intersected the counters. A rather simple procedure proved adequate in accomplishing this. For each mass permutation of each track, the momentum was checked to be sure a particle of the assumed mass could penetrate the 2.9 inch stainless steel chamber body. This imposes a minimum of 740 MeV/c on protons and 235 MeV/c on pions. TVGP had readily available an endpoint co-ordinate for the track as well as the vector momentum. From these values and the magnetic field at the endpoint, a simple helix was constructed and its intersection was found with a cylindrical surface whose radius was equal to the average distance of the

counters from the center of the chamber. If this trial orbit was remotely near to the counters, the magnetic field at the center of the orbit extension was then calculated along with the average momentum after accounting for energy loss, then a new helix was constructed using these values. This refinement was necessary since the magnetic field of the chamber varies more rapidly near its periphery. A final test of this procedure was obtained by integrating a few tracks properly through the magnetic field and noting the magnitude of the deviations from the simple helix approximation. The worst cases deviated by at most a few millimeters, an amount quite adequate for our purposes. However, to prevent losing borderline cases from this effect and to allow for multiple scattering in the stainless steel walls of the chamber, the counters were taken to be a centimeter larger than their true physical size.

Each timing measurement can be divided into three separate parts: $t_1$, the flight time of the beam particle from the production target to the interaction vertex in the bubble chamber; $t_2$, the flight time of the secondary charged particle from the interaction vertex to the counter; and $t_3$, the transit time of light in the scintillator relative to some reference line, nominally the center of the counter. The velocity of the beam particle is derived from the first of these while $t_2$ and $t_3$ can be thought of as corrections to be subtracted from the raw measurement in order to obtain $t_1$. At the close of the extension procedure described above, all the quantities required to calculate $t_2$ and $t_3$ were available: the length of the track from the vertex to its last measured point is supplied by TVGP; the extension procedure yields the arc length from the endpoint to the intersection with the counter, then from the measured momentum we obtain the velocity and hence $t_2$; from the co-ordinates of the intersection of the extended orbit with the counter, we can determine $t_3$. It should be noted that determination of $t_2$ depends on the mass assignment for the track. This at first may appear to be an unfortunate

complication; however it may sometimes be useful in distinguishing the proper mass assignment: at 1 GeV/c pions and protons differ by 0.75 nsec over a 60 cm path, a resolvable difference for large pulse charge.

One expects the distribution of flight times about the mean to be approximately gaussian for these measurements (see Fig. 4 and 5). Since momentum is a rather complicated function of flight time, especially as the particles become increasingly relativistic, it follows that the distribution of momentum about its mean is somewhat skew, and similarly the distribution of curvature $\kappa = 1/(p \cos \lambda)$ (where $\lambda$ is the dip angle in the chamber), which is traditionally used in bubble chamber analysis, is also skew. From these considerations, it seemed appropriate to introduce a new track type into SQUAW which used some variable which was proportional to flight time instead of curvature. A natural choice is the dimensionless quantity $\mu = 1/\beta = c/v$. Since the incident beam track is in other respects a simple two point track (the first point at the production target is edited in, the second is the interaction vertex reconstructed in the chamber), the usual variables of azimuth and slope ($\phi$ and $s = \tan \lambda$) are appropriate to describe its other attributes.

A common procedure in bubble chamber experiments which use charged particles from a momentum analyzed beam is that of editing or averaging the momentum of the incident track just before beginning a kinematical fit. In parallel fashion the new "timing" track type was set up and initialized in parts of SQUAW previously reserved for beam editing. Here, the raw time of flight was corrected for nonlinearity and pulse charge effects as described above, an estimate of the error was made, and the corrections $t_2$ and $t_3$ applied to the refined measurement. If several counters fired, their weighted average $\bar{\tau}$ and its variance $\sigma$ were used:

$$\bar{\tau} = \sum_{i=1}^{n} (\tau_i / \delta\tau_i^2) \cdot \sigma^2 ; \qquad 1/\sigma^2 = \sum_{i=1}^{n} 1/\delta\tau_i^2 .$$

From the surveyed position of the production target and the measured position of

the interaction vertex, the flight distance $\ell$ was calculated. Finally the measured value of $\mu$ could be calculated along with its estimated error. This error was taken to be uncorrelated with any other track co-ordinates in the fit. From this point on, the fit was handled in the standard fashion of SQUAW and delivered at its conclusion a fitted value for $\mu$ which, along with the other track variables, minimized chi-squared for the event as a totality.

One final complication worthy of note arises in the case of multivertex fitting. The correction $t_2$ in cases where particles from a secondary Vee (either $K^o_S$ decay or $\Lambda$ decay) fire the counters involves the flight time of the neutral particle from the interaction vertex to the decay vertex. This can only be calculated with knowledge of the momentum of the neutral and should properly be iterated as the fit proceeds, a procedure which would involve many changes in SQUAW. A less rigorous alternative was taken in which the momentum of the neutral was obtained from a separate three constraint fit of the decay vertex and the correction made using the fitted value for momentum.

## VIII. Logical Selection of Timing Measurements

Some care was required in addition to geometrical considerations in selecting those timing measurements relevant to a particular event. When the extended tracks appeared to have passed through one or more counters, the validity of the time measurements was checked for those counters to assure their being in a physically meaningful range (this guarded against random background or the cases where a particle in passing through a lucite light guide generated prompt signals in advance of legitimate scintillator pulses). Since particles may interact in either liquid hydrogen or the stainless steel chamber body on their way from the last measured track point to a counter, no penalty was exacted when a counter failed to fire although its extended orbit indicated that it should have. After collecting

all valid timing measurements for an event, the firing pattern information (or bunch scaler information where available) was checked for logical consistency. This information tells when during a beam pulse a given TAC fired. Consistency insures that the timing measurements occurred within three beam bunches of one another in the case of the firing pattern and in the same beam bunch in the case of the bunch scalers. Where an inconsistency occurred only timing measurements made in the latest beam bunch were used since early firings could not be associated with the event under consideration. This, of course, presupposes high efficiencies of firing when an orbit appears to pass through a particular counter.

Without a global overview of the whole bubble chamber picture, it is conceivable that three different events could interfere with each other in such a way that wrong timing measurements might be selected. However, since measurement of tracks is required to extend orbits to the counters, this procedure would be quite expensive in measuring time; and further, since the density of events in the chamber is not high with the flux available in the beam knock-out mode of running, the frequency of confusion is indeed small and has been ignored.

## IX. Testing and Results

Since events with no missing neutral particles are of a relatively high constraint class (three constraints at the interaction vertex), analysis of events in this category provides a good measure of the credibility and accuracy of the timing information. If $\tau_{3C}$ is the flight time, $p_{3C}$ the momentum as determined from the three constraint fit, and

$$\beta = p_{3C} / \sqrt{p_{3C}^2 + m^2}$$

simple differentiation yields the formula

$$\frac{d\tau_{3C}}{\tau_{3C}} = (1 - \beta^2) \frac{dp_{3C}}{p_{3C}} .$$

The quantity on the left is the fractional uncertainty of the flight time as determined from the three constraint fit.

For the process

$$n + p \rightarrow p + p + \pi^-$$

the quantity $(dp_{3C}/p_{3C})$ is less than 1% typically at 5 GeV/c and less than 0.5% at 1.5 GeV/c, which values yield $(d\tau_{3C}/\tau_{3C})$ of $3.4 \times 10^{-4}$ and $1.4 \times 10^{-3}$ respectively. For measurement resolution of $\sim 0.5$ nsec, these figures compare with $\lesssim 2.7 \times 10^{-3}$, the value of $(d\tau/\tau)$ as determined directly from the timing measurement. Hence the three constraint fits established the flight time to a better precision over the whole momentum range than the timing measurements and had considerably better precision at the upper end of the momentum interval. Furthermore, the inferred flight times $\tau_{3C}$ are uncorrelated with the direct timing measurements (here denoted $\tau$), and distributions of the quantity $(\tau - \tau_{3C})$ are skewed about zero only from defects in the timing data.

In Fig. 4 the distribution of $(\tau - \tau_{3C})$ is seen for a sample of 1877 events of reaction (1), summarized individually for each counter and combined below in Fig. 5. The centering of the histograms about zero appears true to $\sim 0.1$ nsec and corroborates the validity of the $T_\mu$ and linearity and pulse charge corrections described above. The widths of the curves are an upper bound on the timing resolution (since uncertainty in the fitted momentum and hence in $\tau_{3C}$ contributes to the width). The dashed curve in Fig. 5 is a gaussian with variance 0.75 nsec. It appears to represent the central fall off of the data adequately. The tails of the histogram are substantially above the gaussian and very likely result from a variety of effects such as very low pulse charge and secondary scatters in hydrogen.

The purpose of the timing measurements is, of course, to isolate and study those events where a single neutral particle is present in the final state. Two typical channels amenable to this treatment are

$$n + p \rightarrow p + \pi^+ + \pi^- + n \qquad (2a)$$

$$n + p \rightarrow p + p + \pi^- + \pi^0 \qquad (2b)$$

A simple way of identifying these events, involving only a zero-constraint fit, is to plot the missing mass in each event under the mass assignment assumptions of (2a) and (2b). The missing-mass-squared is, of course, defined to be the square of the difference of the four-momentum between final and initial states, where the beam momentum has been found from time of flight. Where this quantity is large (as in reaction 2a), one may take its square root and plot the mass directly, as is done in Fig. 6. Since the identity of the proton and $\pi^+$ are not a priori known, there are usually two mass combinations for each event which generates an artifically large background. The neutron signal clearly dominates the data.

When the missing particle is less massive, as in reaction 2b, the square of the missing four-momentum may be negative within resolution and one must plot this squared quantity in order to have a variable which behaves well at zero and has uniform resolution. Since both particles are assumed protons, only one combination enters for each event. A sizable peak appears near $m_\pi^2 = 0.0195\ (\text{GeV})^2$ above a 25% background as seen in Fig. 7.

The strength of the signals gives assurance that the one-constraint fits, where the mass of the neutral is fixed, will isolate these two particular channels effectively above a small background. The shaded curves in Fig. 6 and 7 show the same spectra for events with one-constraint fits (only the most probable fit for each event has been plotted).

X. Triggering the Bubble Chamber Flash

Another use of the timing information is in selectively triggering the flash of the bubble chamber only when there are one or more events occurring in a given time region. This is possible with a bubble chamber since the liquid retains track information without serious loss of quality for up to three milliseconds, which is sufficient time to read the counter information into the PDP-9 and evaluate its contents. A portion of the present experiment was run using a triggered flash which required the presence of a timing measurement in the interval 5-38 nsec later than prompt signals (i.e., $T_\mu$ + 5 nsec). This choice corresponds to $K_L^o$ momenta of less than 2 GeV/c and neutron momenta less than 4 GeV/c as seen in the momentum versus flight time plot of Fig. 8. A comparison of the triggered flash and untriggered data is shown in Fig. 9 where spectra for $K_L^o$ decays measured in the chamber (irrespective of whether they fired a counter) are plotted versus the sum of their visible longitudinal momenta. Since these are all three body decays, the undetected neutral particle carries away some of the longitudinal momentum, and hence these spectra are not a true representation of the momentum spectrum of the incident $K_L^o$. Both samples of data contain roughly the same number of events and clearly indicate an increased population in the case of triggering for momenta below 2 GeV/c.

From these data, after some analysis, one can infer the true momentum spectrum of the $K_L^o$ as described in reference (1). These spectra, drawn to the same normalization, are shown in Fig. 10. Once again there is a considerable enhancement of the low momentum portion of the spectrum. Quantitatively one finds an increase of 40% in the flux below 2 GeV/c in the triggered case. In this triggered mode, approximately 25% of the beam pulses gave rise to pictures.

We note here that the act of triggering introduces a bias into the angular

distributions of the low momentum events in the chamber. The limited acceptance of the counter system creates an angular bias for all events with timing information (triggered or not) which is discussed in the next section; but the special effect of triggering is to distort the sample if one uses the bubble chamber measurements alone.

## XI. Conclusions and Physics Application

We conclude that, with some care, a system of counters surrounding a hydrogen bubble chamber can be made to perform precise timing measurements on secondaries emanating from chamber interactions. All the obvious physical obstacles--e.g., piping scintillation light out of the region of high magnetic field, shielding phototubes in a large fringe field, and monitoring and maintaining the stability of the system over the duration of an experiment--can be adequately surmounted. The new measurements are easily incorporated into the picture analysis cycle and easily tested by studying final states without neutrals.

If the bubble chamber had been expressly designed to accommodate a system of counters of this sort, some of the physical problems might have been alleviated. In particular, the necessity of placing our light guides so near the downstream beam and chamber secondaries made our measurements unnecessarily vulnerable to background from Cerenkov radiation. Slight design changes in the chamber body and vacuum tank assembly could easily have increased the solid angle acceptance by a substantial amount and would have greatly simplified installation of the system.

The solid angle limitation is common to nearly all high energy physics detectors; the bubble chamber is somewhat unique, in fact, in its ability to detect nearly all charged particles in a $4\pi$ geometry. The time of flight information

has been bought to some extent at the expense of this unique feature but hopefully not at the expense of the ability to measure cross sections.

Two methods may be used against this problem. If sufficient solid angle is covered so that every possible final state has a non-zero detection probability, then using Monte Carlo techniques one can calculate a weight for each detected event which corrects properly for geometrical losses. In this particular experiment we can check the technique by studying the 3-C channel (1). In the momentum interval 1.5 to 5.0 GeV/c, which corresponds to our timing gate, we find 94% of the events have efficiencies greater than 0.10 and less than 1% have efficiencies below 0.01. Since pions are more penetrating than protons, channel (2a) (where we cannot check the efficiency distribution directly) should have generally higher efficiencies.

If the above weighting technique cannot be used, the data may be compared with various models by integrating the predicted partial cross sections over the acceptance of the apparatus. This treatment is less appealing since it presupposes the existence of good models for the interaction.

Currently we are studying channel (2a) where both these approaches can be used. This particular final state has a relatively large cross section which is approximately constant with energy. The process is dominated by $\Delta^{++}$ (1236) - $\Delta^{-}$ (1236) production which we hope to study as a function of energy. Previous work on this final state has been done in deuterium where the nuclear binding of the neutron has made interpretation of the results difficult. Our direct study, made possible by time of flight, should resolve these difficulties.

Acknowledgements

The successful construction and operation of this system would not have been

possible without the dedicated efforts of a great many individuals and groups, too numerous to mention. The contributions of the following were particularly essential to this work; Arpad Barna, Burnett Specht, and Ron Stickley assisted greatly in early development studies. We are indebted to the crew of the 40" bubble chamber, under the direction of Robert Watt, for their co-operation and patience and especially to Gerard Putallaz who designed the brackets and feed throughs for the counters to fit in the restricted vacuum tank. The Injection group of Accelerator Physics, under the direction of Drs. Gred A. Loew and Roger Miller, was responsible for the success of the beam knock out system and the Beam Pick Off timing detector. We also wish to thank Kerry D. Mauro who did much of the work required to interface the computer with the electronics and Donald McShurley who spent long hours both fabricating the scintillation counters and designing and building many of the special electronics components required for the system. Finally we are indebted to the other members of the group who worked on the $K^0$ experiment, particularly Dr. James S. Loos who was responsible for the secondary beam during the data-taking phase of this experiment and who assisted greatly with the counter checkout.

References


1. A. D. Brody, et al., Phys. Rev. Letters 22, 966 (1969); G. W. Brandenberg, et al., Phys. Rev. D 7, 6 (1973).
2. W. M. Smart and D. W. G. S. Leith, Group B Physics Note 26, unpublished, (1969).
3. R. G. Friday and K. D. Mauro, IEEE Transactions on Nuclear Science NS-19, No. 1, 726 (1972).
4. F. T. Solmitz, A. D. Johnson, and I. B. Day, Three View Geometry Program, Alvarez Group Programming Note P-117; O. I Dahl, T. B. Day, F. T. Solmitz, and N. L. Grould, SQUAW, Group A Programming Note P-126 (unpublished).

Figure Captions

1. A drawing of SLAC 40" bubble chamber showing the hydrogen vessel, vacuum tank, and magnet yoke. The positions of the scintillators, fiber optics, light pipes, and photomultiplier tubes are indicated.
2. A simplified block drawing of the scintillation counter data acquisition system, showing schematically how it was used to measure beam momentum for a $K^o_L$ beam.
3. Block diagram of the fast electronics used to measure time and pulse charge for one of the 12 counters.
4. Distributions for each counter of measured time minus $\tau_{3C}$, the time inferred from three constraint kinematic fits to the HBC measurements.
5. Distribution of $\tau - \tau_{3C}$ summed for all counters. The dashed curve is a gaussian with variance 0.75 nsec shown for comparison.
6. Distribution of missing mass assuming p, $\pi^+$, and $\pi^-$ for charged particles in the final state, the shaded histogram shows events whose most probable one constraint fit was to the hypothesis $np \rightarrow p\pi^+\pi^-n$.
7. Distribution of missing mass squared assuming p, $\pi^-$, and p for charged, final-state particles. The shaded curve shows events with a most probable fit to $np \rightarrow p\pi^-p\pi^+$.
8. Momentum versus time late for neutrons and $K^o_L$.
9. Distribution of the visible longitudinal momentum for $K^o_L$ decays for (a) untriggered running conditions and (b) conditions where the chamber flash was triggered only when there was a beam particle with a time late greater than 5 nsec.
10. Momentum spectrum for $K^o_L$ mesons under triggered and untriggered running conditions. These spectra are inferred from the data in Fig. 9 as described in reference (1).

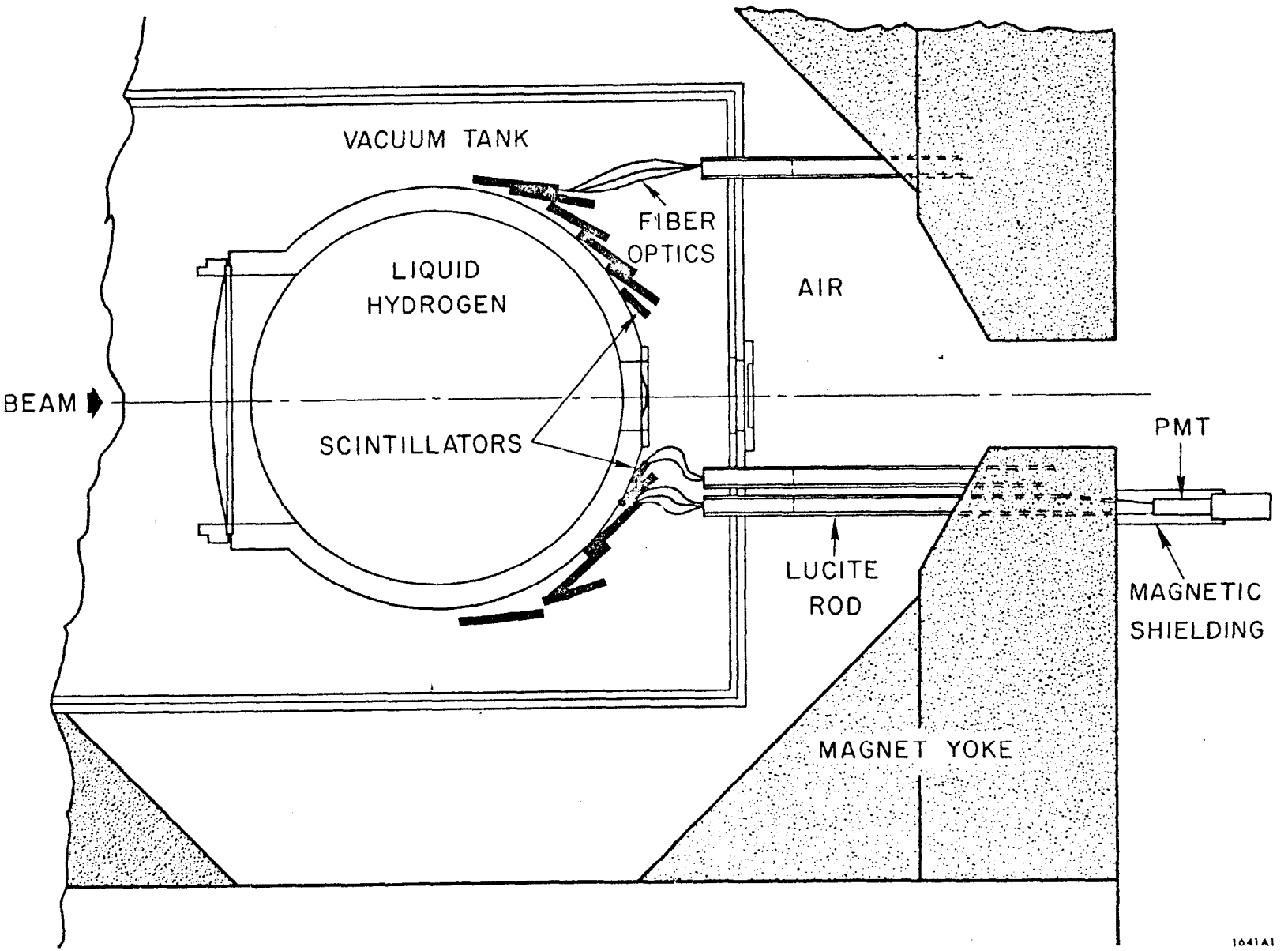
VACUUM TANK
FIBER
OPTICS
LIQUID
HYDROGEN
AIR
BEAM
SCINTILLATORS
PMT
LUCITE
ROD
MAGNETIC
SHIELDING
MAGNET YOKE
1041A1

FIG. 1

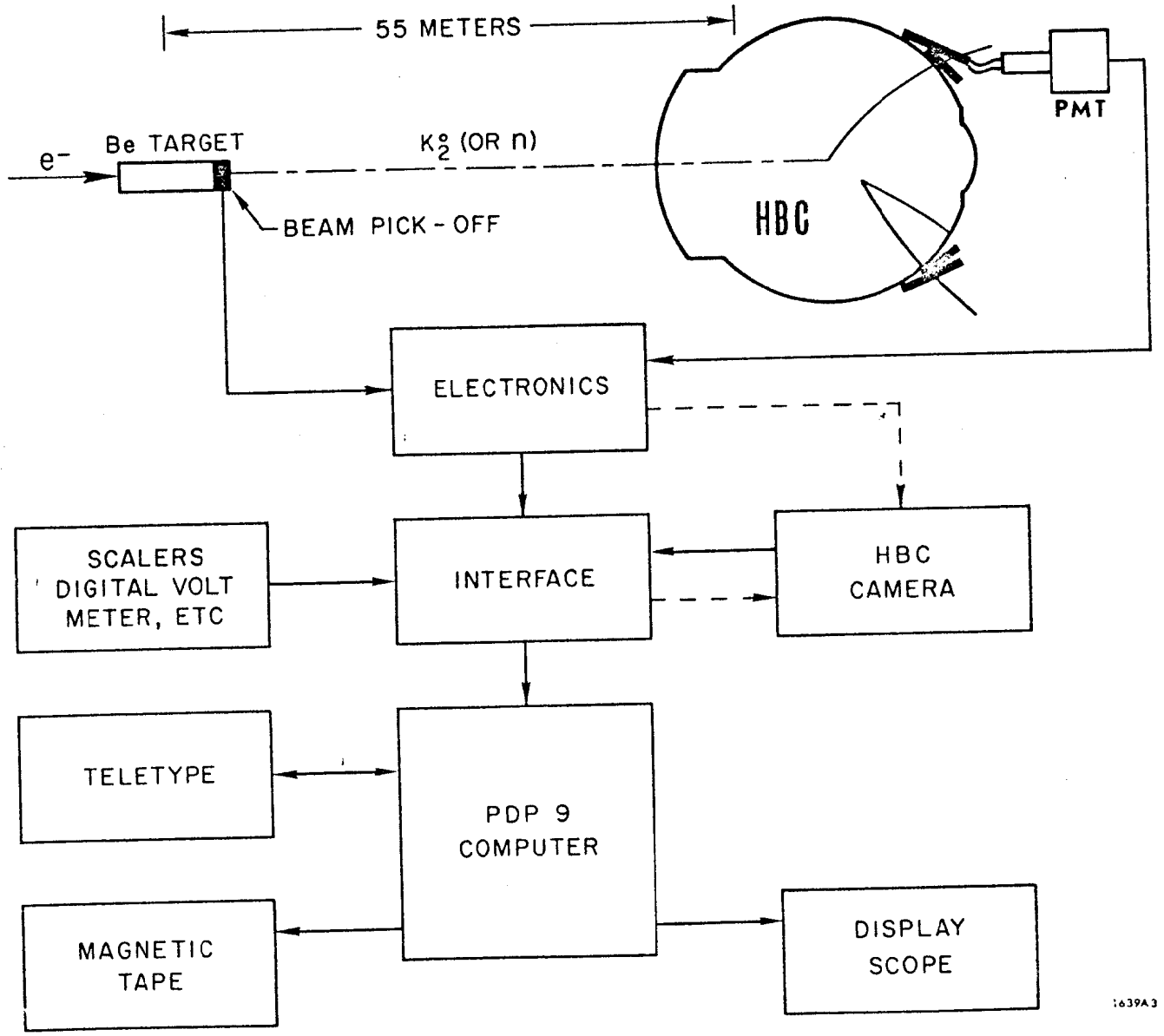
55 METERS
PMT
e⁻
Be TARGET
$K_2^0$ (OR n)
HBC
BEAM PICK - OFF
ELECTRONICS
SCALERS
DIGITAL VOLT
METER, ETC
INTERFACE
HBC
CAMERA
TELETYPE
PDP 9
COMPUTER
MAGNETIC
TAPE
DISPLAY
SCOPE
1639A3

FIG. 2

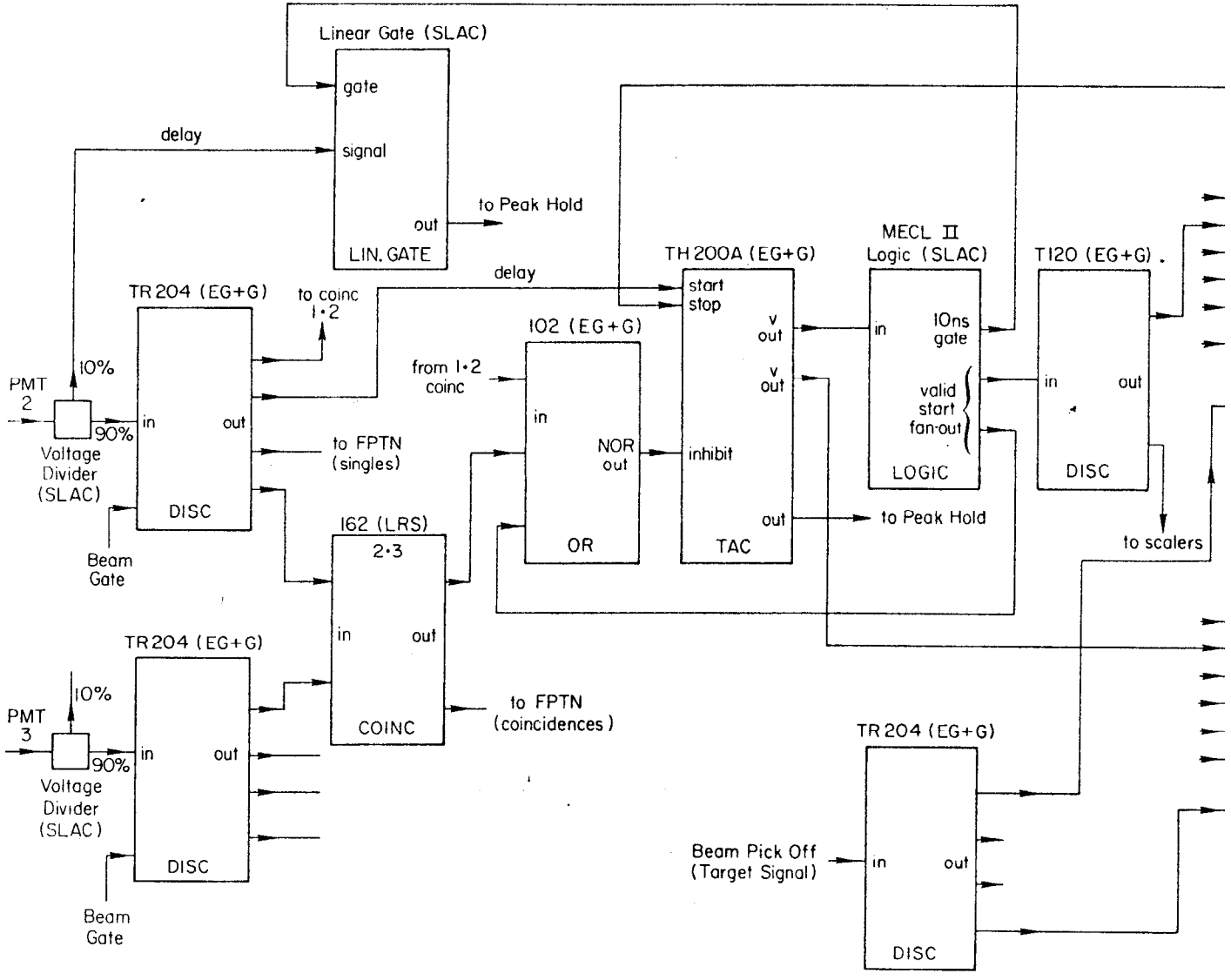
Linear Gate (SLAC)
gate
signal
out
LIN. GATE
delay
to Peak Hold
TH 200A (EG+G)
start
stop
v out
v out
inhibit
out
TAC
MECL II
Logic (SLAC)
in
10ns gate
valid start fan-out
LOGIC
T120 (EG+G)
in
out
DISC
delay
TR 204 (EG+G)
to coinc 1·2
10%
PMT 2
90%
Voltage Divider (SLAC)
in
out
DISC
Beam Gate
to FPTN (singles)
102 (EG+G)
from 1·2 coinc
in
NOR out
OR
to Peak Hold
to scalers
162 (LRS)
2·3
in
out
COINC
to FPTN (coincidences)
TR 204 (EG+G)
10%
PMT 3
90%
Voltage Divider (SLAC)
in
out
DISC
Beam Gate
TR 204 (EG+G)
Beam Pick Off (Target Signal)
in
out
DISC

FIG. 3

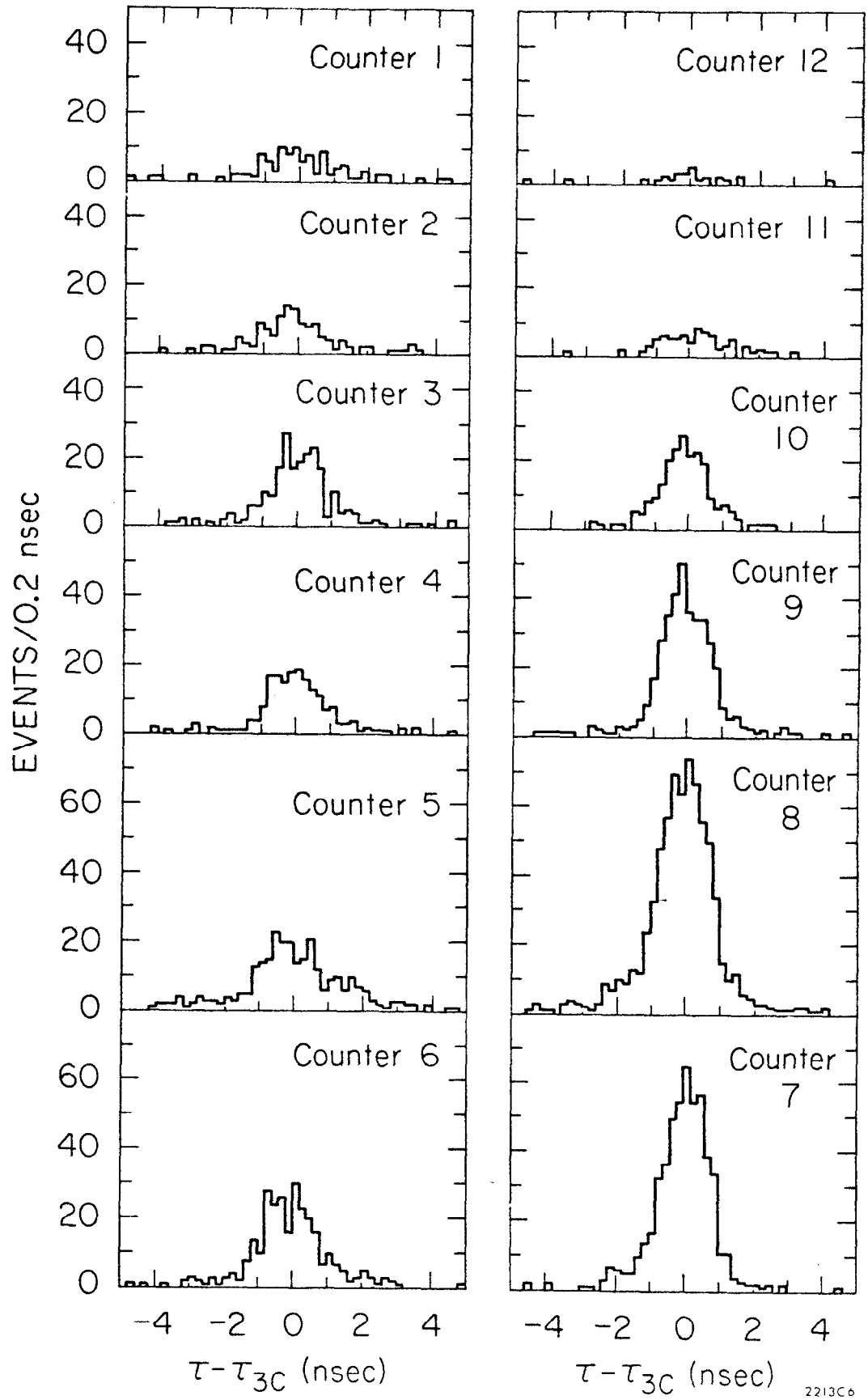
Counter 1
Counter 2
Counter 3
Counter 4
Counter 5
Counter 6
Counter 12
Counter 11
Counter 10
Counter 9
Counter 8
Counter 7
EVENTS/0.2 nsec
$\tau - \tau_{3C}$ (nsec)
$\tau - \tau_{3C}$ (nsec)
2213C6

FIG. 4

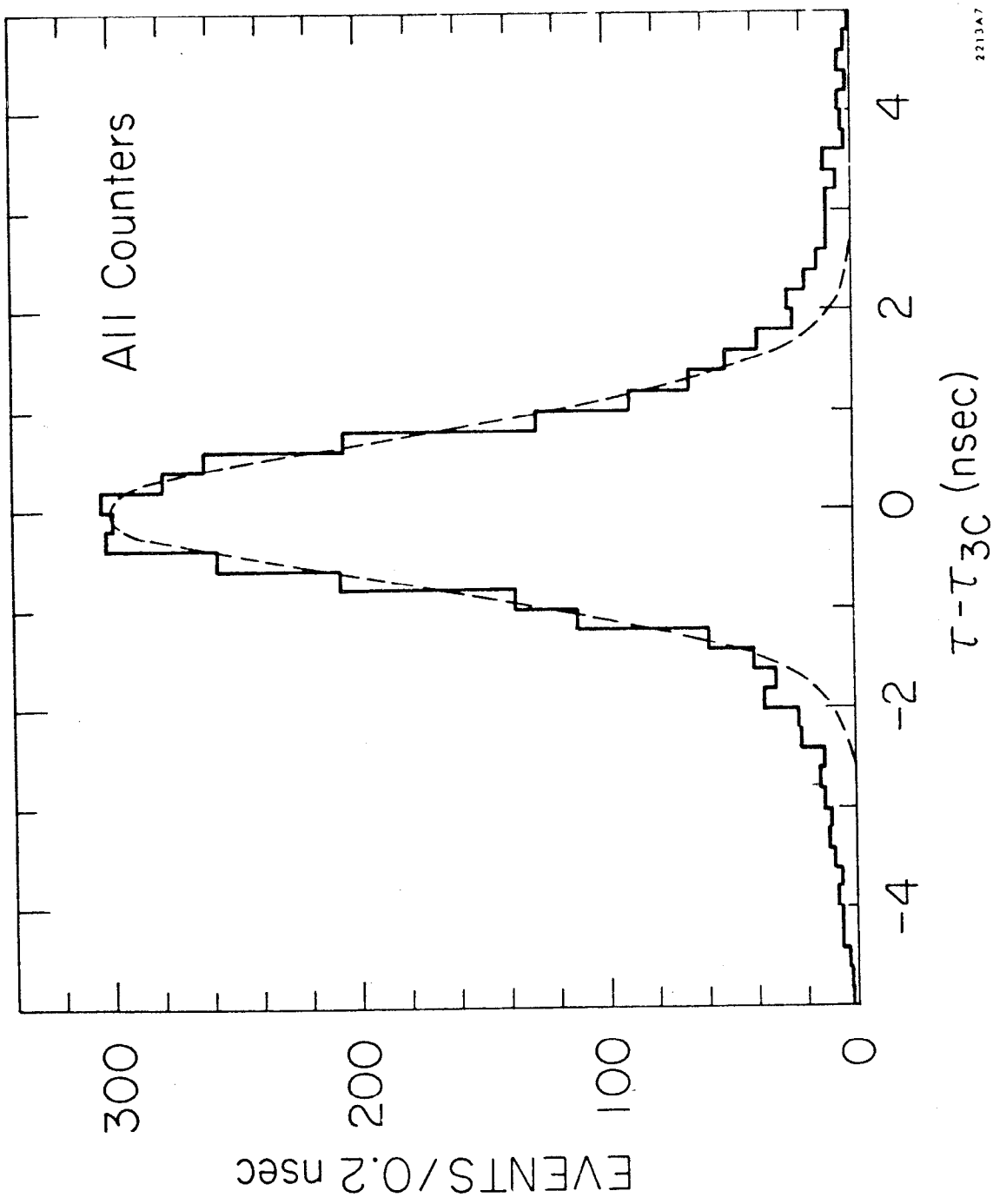
All Counters
EVENTS/0.2 nsec
300
200
100
0
-4
-2
0
2
4
$\tau - \tau_{3C}$ (nsec)
221347

FIG. 5

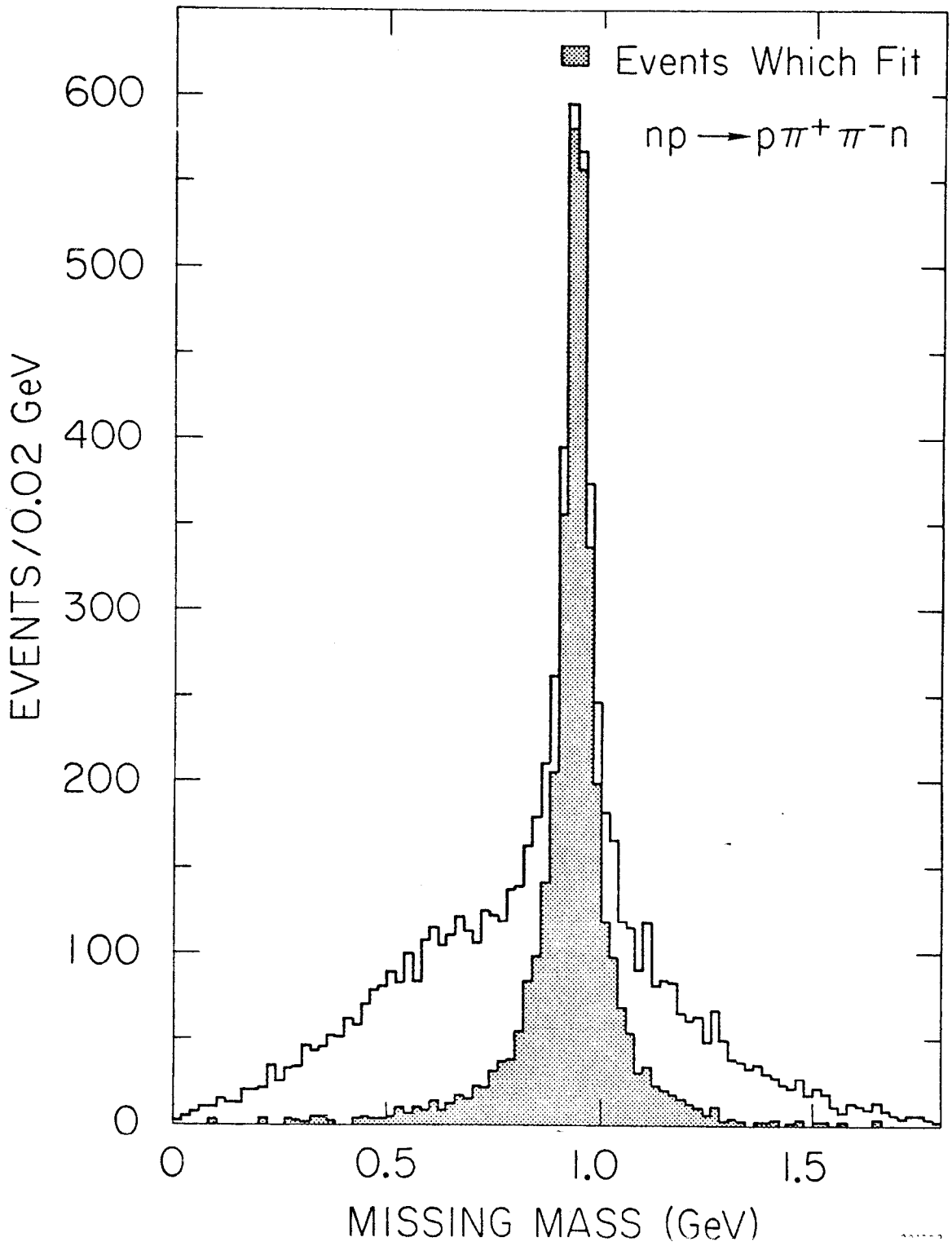
Events Which Fit
$np \rightarrow p\pi^+\pi^-n$
600
500
400
300
200
100
0
EVENTS/0.02 GeV
0
0.5
1.0
1.5
MISSING MASS (GeV)

FIG. 6

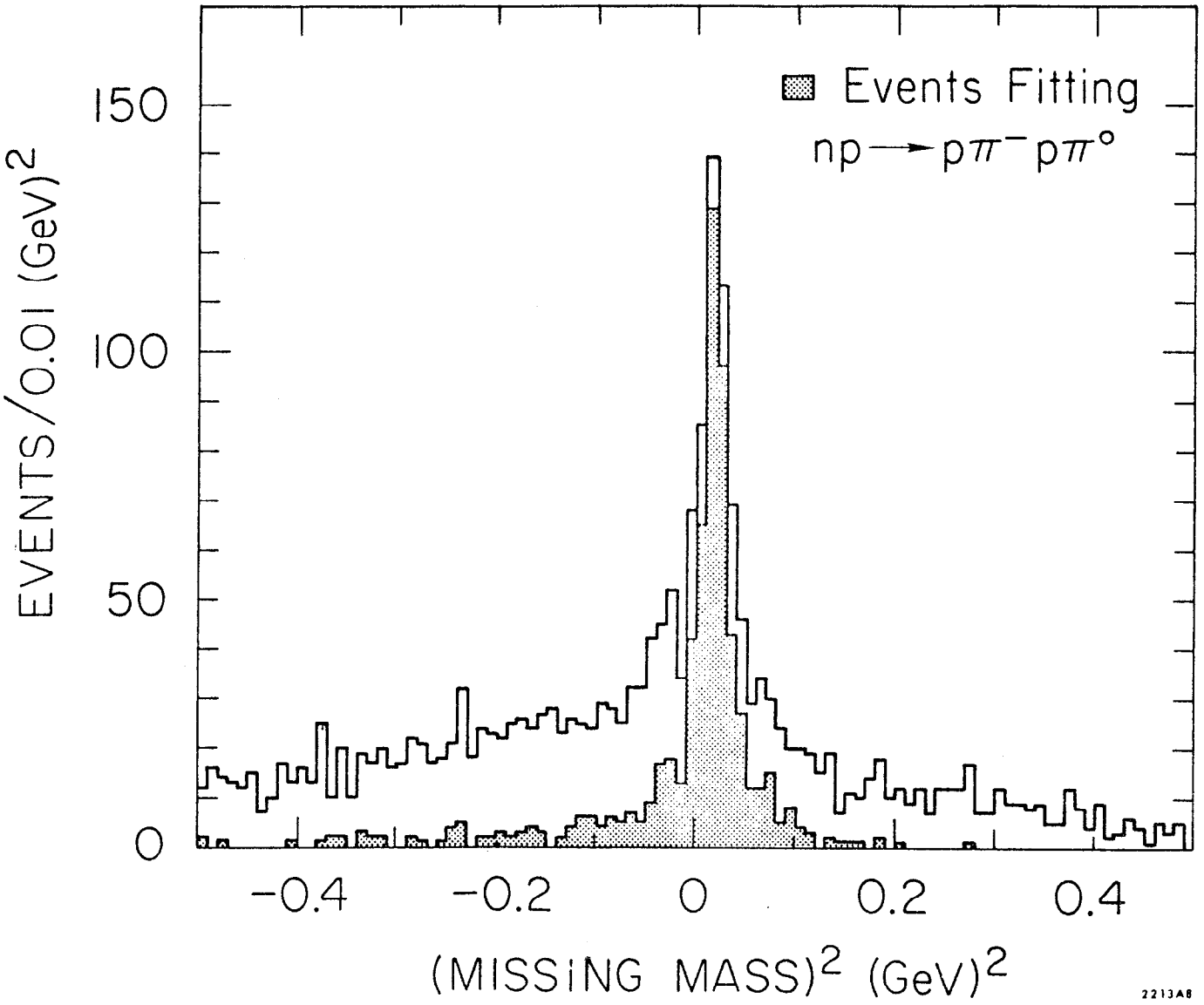
Events Fitting
np → pπ⁻pπ°
EVENTS/0.01 (GeV)²
150
100
50
0
-0.4
-0.2
0
0.2
0.4
(MISSING MASS)² (GeV)²
2213A8

FIG. 7

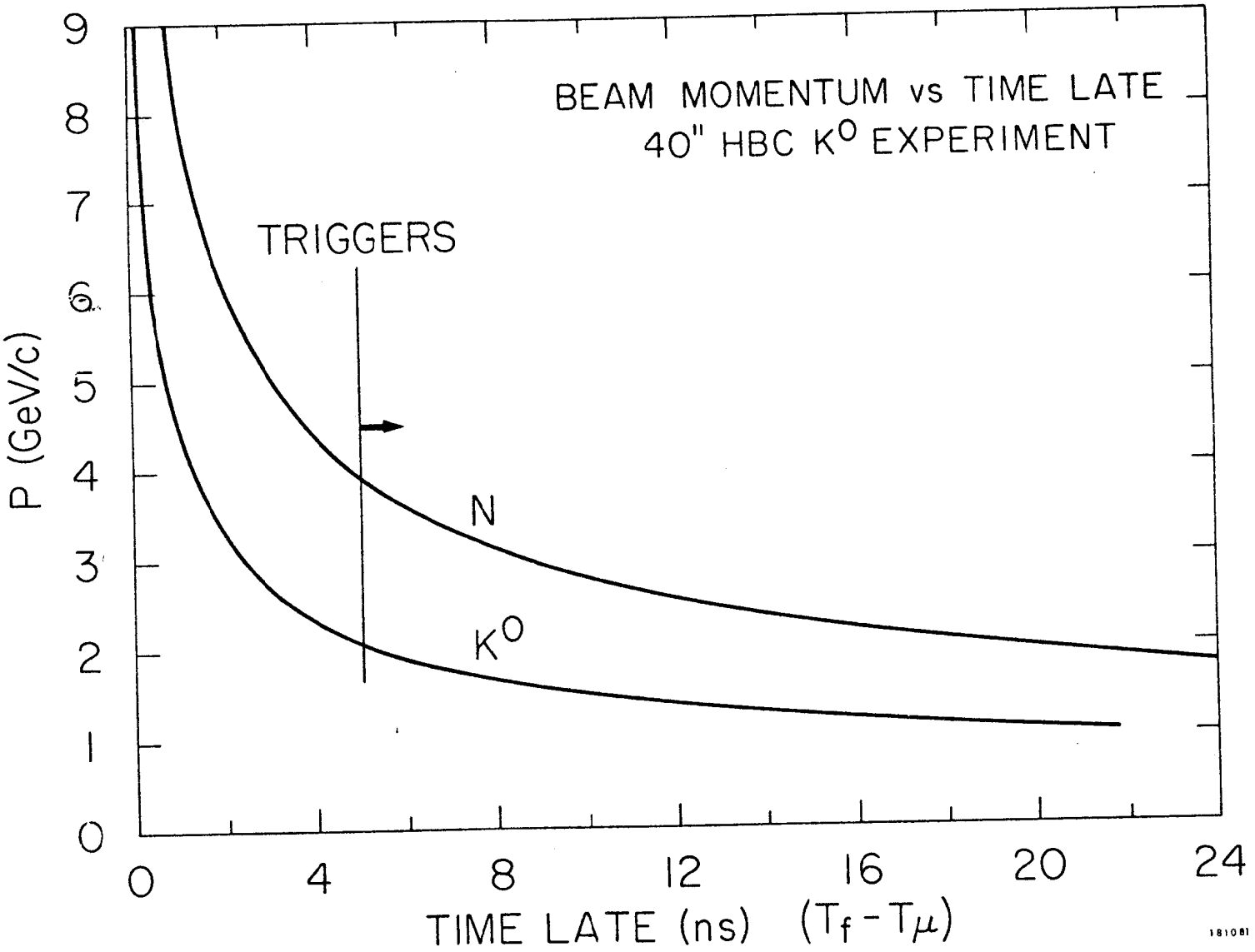
BEAM MOMENTUM vs TIME LATE
40" HBC K⁰ EXPERIMENT
TRIGGERS
N
K⁰
P (GeV/c)
TIME LATE (ns) (Tf - Tμ)
0
1
2
3
4
5
6
7
8
9
0
4
8
12
16
20
24
181081

Fig. 8

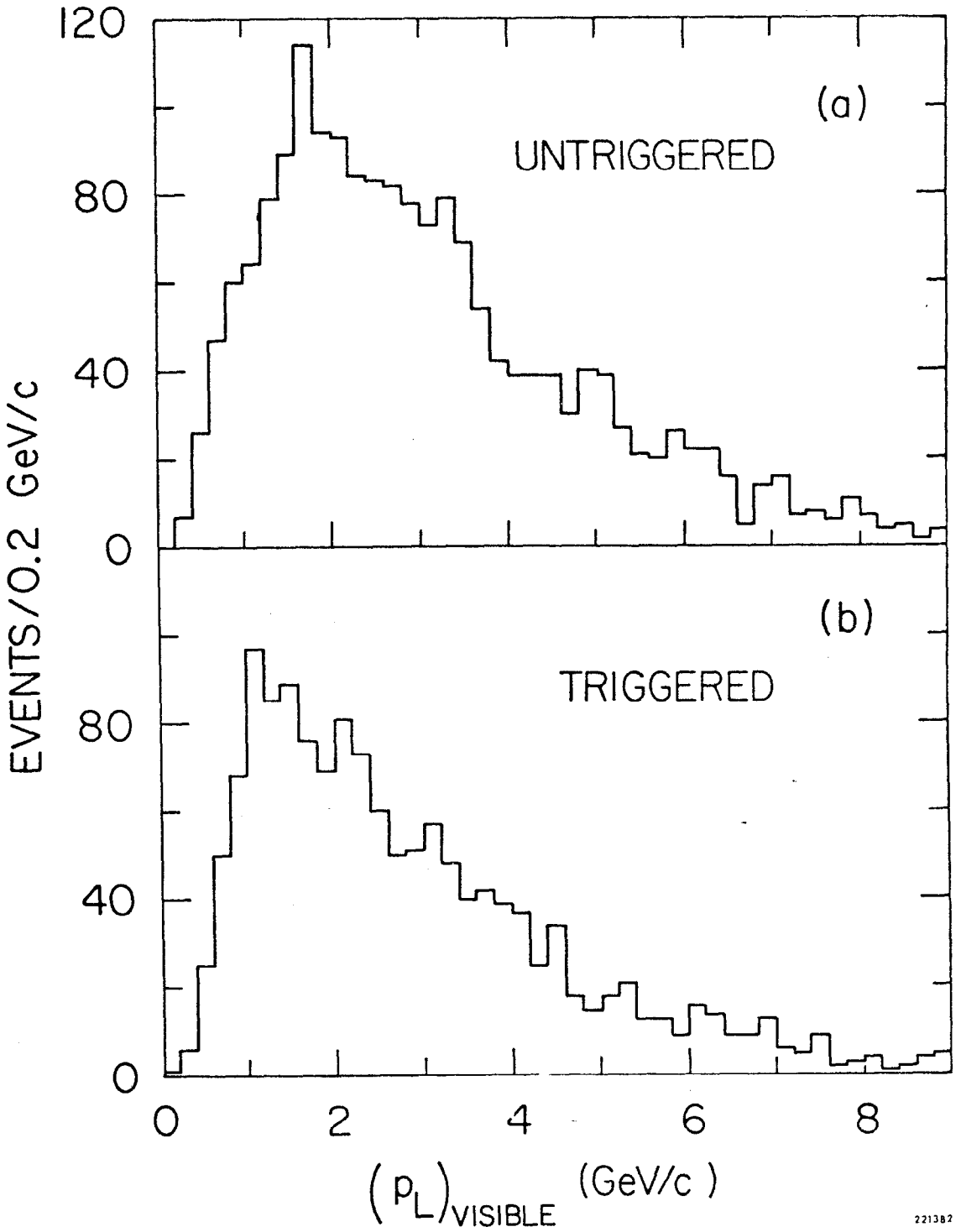
120
80
40
0
(a)
UNTRIGGERED
80
40
0
(b)
TRIGGERED
EVENTS/0.2 GeV/c
0
2
4
6
8
$(p_L)_{VISIBLE}$ (GeV/c)
221382

FIG. 9

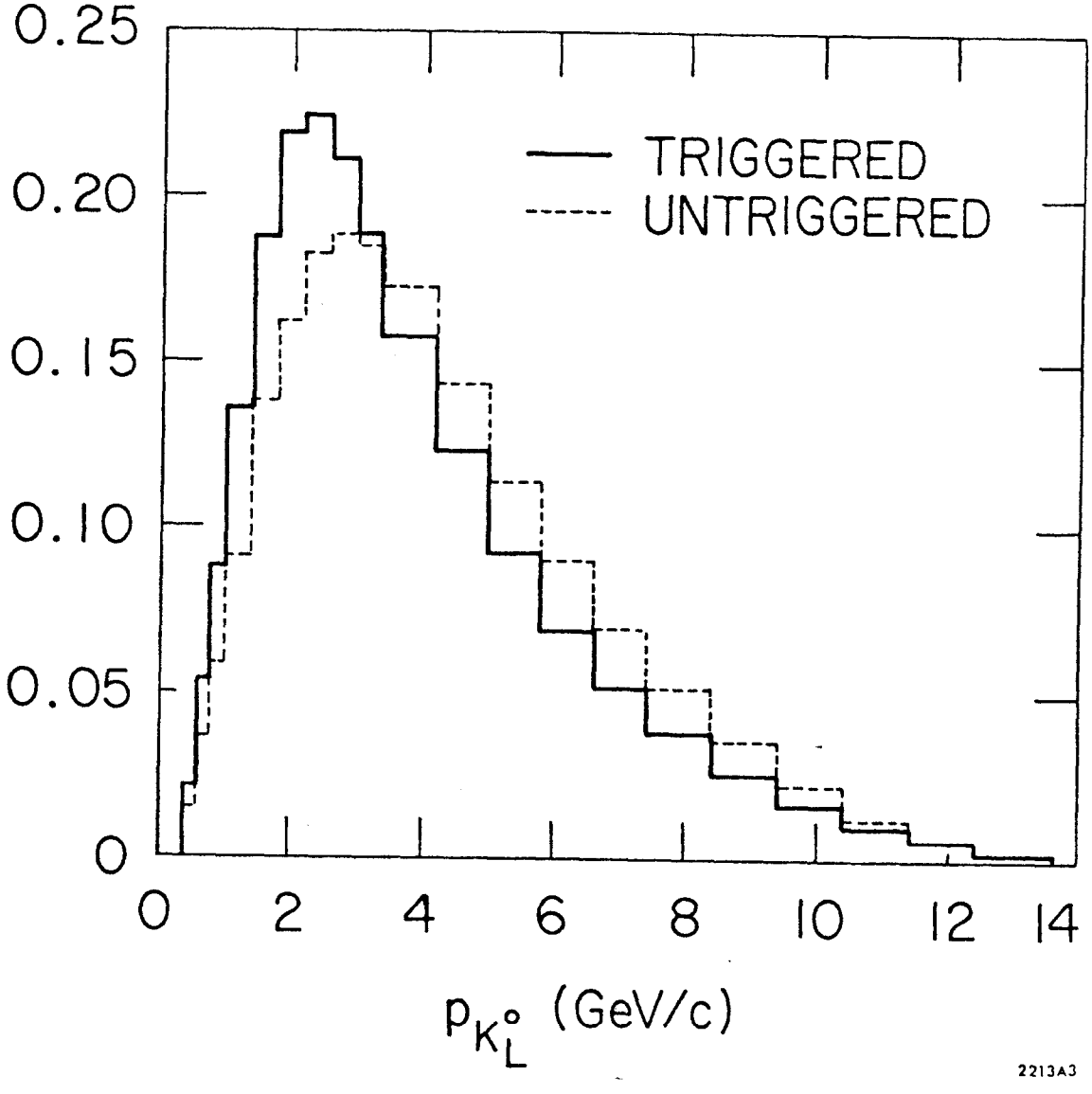
0.25
0.20
0.15
0.10
0.05
0
TRIGGERED
UNTRIGGERED
0
2
4
6
8
10
12
14
$p_{K_L^0}$ (GeV/c)
2213A3

FIG. 10